

Article

Self-Consistent Two-Gap Description of MgB₂ Superconductor

Hyunsoo Kim ^{1,2,†} , Kyuil Cho ¹ , Makariy A. Tanatar ^{1,2}, Valentin Taufour ^{1,‡}, Stella K. Kim ^{1,2}, Sergey L. Bud'ko ^{1,2}, Paul C. Canfield ^{1,2}, Vladimir G. Kogan ¹ and Ruslan Prozorov ^{1,2,*}

¹ Ames Laboratory, Ames, IA 50011, USA

² Department of Physics & Astronomy, Iowa State University, Ames, IA 50011, USA

* Correspondence: prozorov@ameslab.gov

† Current address: Center for Nanophysics and Advanced Materials, University of Maryland, College Park, MD 20742, USA.

‡ Current address: Department of Physics, University of California Davis, Davis, CA 95616, USA.

Received: 18 June 2019; Accepted: 2 August 2019; Published: 6 August 2019



Abstract: A self-consistent two-gap γ -model is used to quantitatively describe several thermodynamic properties of MgB₂ superconductor. The superconducting coupling matrix, v_{ij} , was obtained from the fitting of the superfluid density in the entire superconducting temperature range. Using this input, temperature-dependent superconducting gaps, specific heat, and upper critical fields were calculated with no adjustable parameters and compared with the experimental data as well as with the first-principles calculations. The observed agreement between fit and data shows that γ -model provides adequate quantitative description of the two-gap superconductivity in MgB₂ and may serve as a relatively simple and versatile self-consistent description of the thermodynamic quantities in multi-gap superconductors.

Keywords: superconducting gap symmetry and structure; penetration depth; band structure of superconductors

1. Introduction

Discovery of superconductivity in MgB₂ triggered significant interest for its highest superconducting transition temperature, $T_c \approx 39.2$ K, among “conventional” superconductors with phonon-mediated pairing [1–4]. The conventional pairing mechanism was strongly supported by the Boron isotope effect [5–7] and exponential low-temperature attenuation of the thermodynamic quantities upon cooling indicating nodeless order parameter. Such high T_c and isotropic nature of the superconducting gap offer excellent opportunities for various technological applications, including superconducting magnets, radio frequency resonance cavities for electron accelerators [8], and the next generation information technology, including high-frequency metamaterials, quantum integrated circuits, and quantum processing [9,10].

From the fundamental physics point of view, it was realized that a multi-band, multi-gap superconductivity model is required to explain the observed full-temperature range variation of thermodynamic properties. Smaller than expected for a single-gap superconductor exponential tail and a characteristic hump below T_c in specific heat vs. temperature, $C(T)$, prompted the use of a well-known phenomenological α -model, used to describe strong-coupling superconductivity [11]. In the original model, $\alpha = \Delta(T)/\Delta_{BCS}(0)$, where Bardeen–Cooper–Schrieffer isotropic weak-coupling single-band value is $\Delta_{BCS}(0)/T_c \approx 1.763$. Then $\alpha \geq 1$ was used to effectively vary the coupling strength. Indeed, this procedure is not self-consistent, but in the case of a single-band superconductor the actual temperature dependence of $\Delta(T)$ was not too far from $\Delta_{BCS}(T)$. In case of MgB₂, two gaps

were assumed to have the same, BCS temperature dependencies, but their amplitudes were taken as free parameters to fit the $C(T)$ data [12–15] and, later, London penetration depth [16–18]. The third parameter was the relative contributions from each band, proportional to the partial density of states and average Fermi velocities. Analysis of angle resolved photoemission spectroscopy data (ARPES) finds the difference in electron–phonon coupling between σ and π bands supporting two-band superconductivity in MgB_2 [19–21].

While this simple approach “worked” in practice and has been widely used even to-date to describe multi-band superconductivity, it is not self-consistent and the obtained parameters have no physical significance. Indeed, it has been realized right away and more elaborate models were used. Whereas original α -model used weak-coupling BCS gaps [13], later refinements used temperature dependent gaps calculated microscopically for MgB_2 [22], but then again used the ratio of the gap amplitudes and the relative contributions from different bands as free parameters to fit the experimental data. While such exercise surely points toward multi-gap superconductivity in MgB_2 , it cannot provide information regarding superconducting pairing matrix and the success of α -model is mostly due to the fact that thermodynamic quantities do not exhibit sharp features as a function of temperature and that in MgB_2 interband coupling is quite significant.

Being clearly the case in MgB_2 , multiband superconductivity has received significant attention and led to the re-evaluation of known systems and looking for novel materials. Surely enough, it turned out that it is much more common if not ubiquitous with the prominent example of a diverse family of iron based superconductors [23–26], heavy fermions [27] and even elemental lead [28]. Full microscopic calculations based on multiband Eliashberg arbitrary coupling were performed, but using them to fit the experimental data was not feasible due to complexity of the realistic electronic structure as well as the number of the parameters involved [14,29,30]. Therefore, relatively simple, but self-consistent, approach was needed and such description, called the γ -model, was introduced based on Eilenberger formulation of the Gor’kov equations [31], and it provided a direct path to evaluation of the coupling constants from the data [32]. We used this model to describe multi-band superconductivity in various iron-based superconductors [24]. Originally, two isotropic s-wave gaps in the clean limit are considered. Later it was generalized for several anisotropic gaps to describe superconductivity in FeSe [33]. It can also be adopted to include scattering, but then the number of unknown parameters becomes too large. In the clean case, provided that bandstructure with Fermi velocities and partial densities of states are known, the unknown coupling matrix can be determined by fixing one of the elements to match the experimental superconducting transition temperature, T_c , and varying others to fit experimental quantity as a function of temperature. The quantity can be, for example, specific heat or superfluid density. Once the interaction matrix is obtained, all other thermodynamic quantities, including free energy, thermal conductivity and critical fields, can be calculated. This provides a physically meaningful way to test the model against several independent measurements.

In this work, we used a self-consistent γ -model to describe superconducting properties of MgB_2 and successfully obtained the interaction matrix by fitting its normalized superfluid density measured in a purest MgB_2 single crystal up to date, which was grown out of molten Mg at high pressure. The superb quality of the sample guarantees the most reliable temperature-dependent London penetration depth. Using the obtained *single set* of fitting parameters, the thermodynamic quantities including specific heat and upper critical field were calculated, and the temperature dependence of order parameters is in good agreement with the spectroscopic tunneling experiments.

2. Results and Discussion

Figure 1a shows temperature dependent normalized magnetic moment, $M(T)/M_{\text{ZFC}}(5\text{ K})$, measured on warming after a 10 Oe magnetic field was applied at 5 K (zero-field cooling (ZFC)) and then on cooling without turning the field off (field-cooling (FC)). The normalization was performed to estimate the amount of the expelled flux from the sample interior (unknown demagnetization

correction does not allow for the determination of absolute magnetic susceptibility). Figure 1b shows magnetic moment as a function of magnetic field in MgB₂ crystal measured at 5 K. Sharp superconducting transition, substantial (50%) Meissner expulsion and virtually no magnetic hysteresis indicate low pinning and overall very clean superconducting nature of this sample.

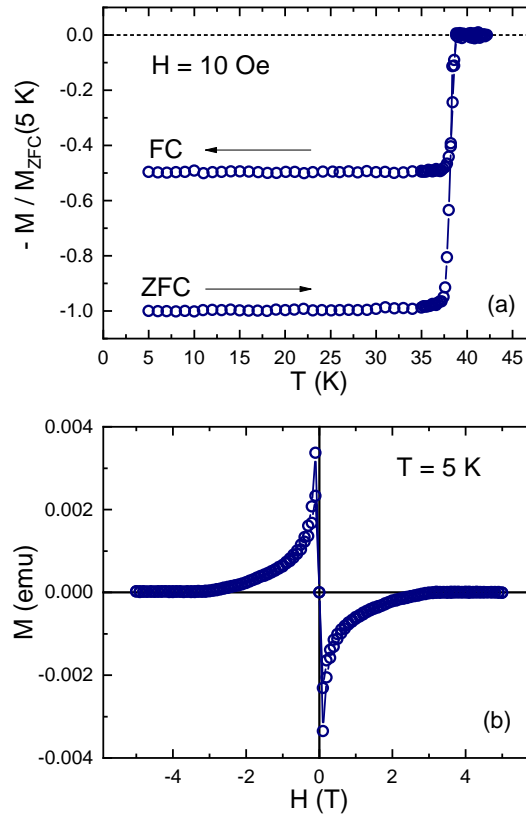


Figure 1. (a) Normalized magnetic moment, $M(T)/M_{ZFC}(5\text{ K})$, measured after cooling in zero magnetic field to 5 K, applying $H_{DC} = 10\text{ Oe}$ and then measuring on warming (zero-field cooling (ZFC)) above T_c and then on cooling (field-cooling (FC)). (b) Magnetization loop, $M(H)$, in MgB₂ crystal measured at 5 K.

Figure 2 shows the temperature variation of London penetration depth $\Delta\lambda(T)$ in the same crystal of MgB₂ used for the magnetic susceptibility measurements shown in Figure 1. The inset shows $\Delta\lambda(T)$ over the entire superconducting temperature range, which exhibits a sharp transition at $T_c = 39\text{ K}$. In the main panel, the low temperature part of $\Delta\lambda(T)$ up to $0.3T_c$ was shown and fitted to the s -wave BCS model, $\Delta\lambda(T) = \lambda(0)\sqrt{\pi\Delta(0)/2k_B T} \exp(-\Delta(0)/k_B T)$, with $\lambda(0)$ and $\Delta(0)$ being the fitting parameters. The best fitting curve shown by solid curve can be achieved with $\lambda(0) = 65 \pm 1\text{ nm}$ and $\Delta(0)/k_B T_c = 0.71 \pm 0.01$. Although the fitting to a single-gap s -wave BCS function is reasonable, the $\lambda(0)$ obtained is much smaller than values in literature, which ranges between 84 and 116 nm [17,22,34,35]. Notably, the gap amplitude is smaller than a weak-coupling value of $\Delta(0)/k_B T_c = 1.76$ [2], which is impossible in a single gap system. In fact, these deviations indicate either anisotropic superconducting gap or presence of multiple gaps [24,36].

In order to investigate the multi-gap nature in MgB₂, normalized superfluid density, $\rho_s = \lambda^2(0)/\lambda^2(T)$, was calculated using $\lambda(0) = 100\text{ nm}$, approximate average from Ref. [17,22,34,35]. The experimental superfluid density shown by symbols in Figure 3a was fitted to $\rho_s = \gamma\rho_1 + (1 - \gamma)\rho_2$ by using the self-consistent γ -model [32]. Here $\gamma = n_1 v_1^2 / (n_1 v_1^2 + n_2 v_2^2)$, where $v_1^2 = 3.3 \times 10^{15}\text{ cm}^2/\text{s}^2$ and $v_2^2 = 2.3 \times 10^{15}\text{ cm}^2/\text{s}^2$ are averages over corresponding band of the squared in-plane Fermi velocities and n_i are normalized partial densities of states per spin, $n_1 = 0.44$ and $n_2 = 1 - n_1$ [37]. During the fitting, one of the in-band interaction parameters, λ_{11} ,

is adjusted to produce close to experimental transition temperature, $T_c = 39$ K after convergence of the fit. A phonon-mediated superconductivity with Debye temperature of 750 K was assumed in calculations of T_c . The only two free parameters are λ_{12} and λ_{22} . During the fitting, superconducting gaps were obtained self-consistently. Their temperature dependence is shown in Figure 3b by solid lines. Experimentally determined gaps from tunneling spectroscopy [38] are shown by symbols for comparison.

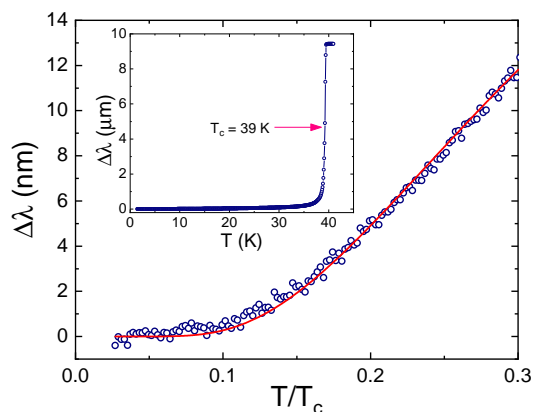


Figure 2. Temperature variation of London penetration depth $\Delta\lambda(T)$ in MgB_2 . Inset: $\Delta\lambda(T)$ over the full temperature range. Main panel: low-temperature part of experimental $\Delta\lambda(T)$ (symbols). Solid curve is the best fitting to a single-gap s -wave BCS asymptotic behavior, $\Delta\lambda(T) = \lambda(0)\sqrt{\pi\Delta(0)/2k_B T} \exp(-\Delta(0)/k_B T)$ with $\lambda(0)$ and $\Delta(0)$ as fitting parameters within “low-temperature” range up to $0.3T_c$.

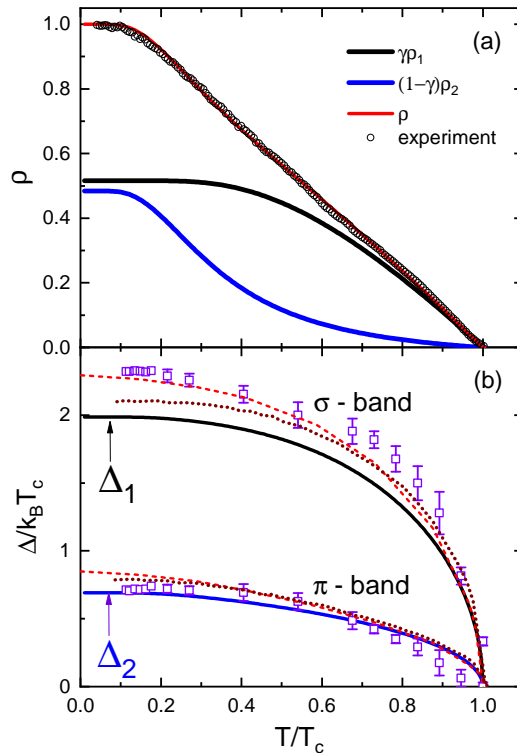


Figure 3. (a) Fitting of the experimental superfluid density, $\rho_s = \lambda^2(0)/\lambda^2(T)$ (symbols), to the γ -model (lines). Partial superfluid densities, $\gamma\rho_1$ and $(1-\gamma)\rho_2$ are also shown. (b) Temperature dependent superconducting energy gaps $\Delta_1(T)/k_B T_c$ and $\Delta_2(T)/k_B T_c$ calculated from the fitting procedure (lines). These results are compared with the experimental tunneling spectroscopy results [38] (purple open squares) and theoretical estimates [29] (red dashed lines), [30] (brown dotted lines).

Specific heat was deduced by using the fit parameters from the γ -model fit of superfluid density and plotted in Figure 4. It is quantitatively consistent with the experimental data [39] and estimate from the first principles calculation [30].

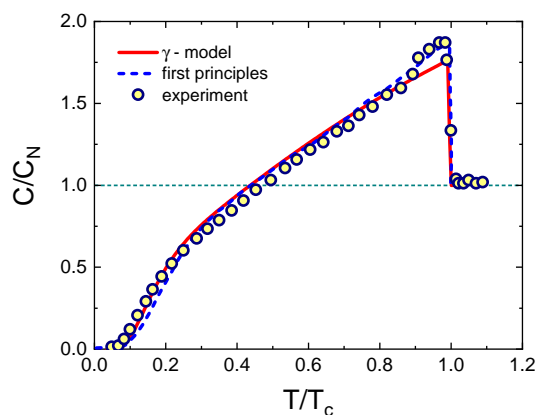


Figure 4. Temperature dependent specific heat C/C_N in MgB_2 . Solid line and symbols represent a calculated result by using γ model [32] and an experimental work by Putti et al. [39], respectively. The dotted line represents the estimate from first principles calculation [30].

Finally, we use parameters of the γ -model determined from the fitting of superfluid density, to calculate the upper critical field in the clean limit following ref. [40]. Temperature dependent upper critical fields were deduced for both field parallel and perpendicular to the in-plane and plotted in Figure 5. The results were quantitatively consistent with other experimental data [41–43].

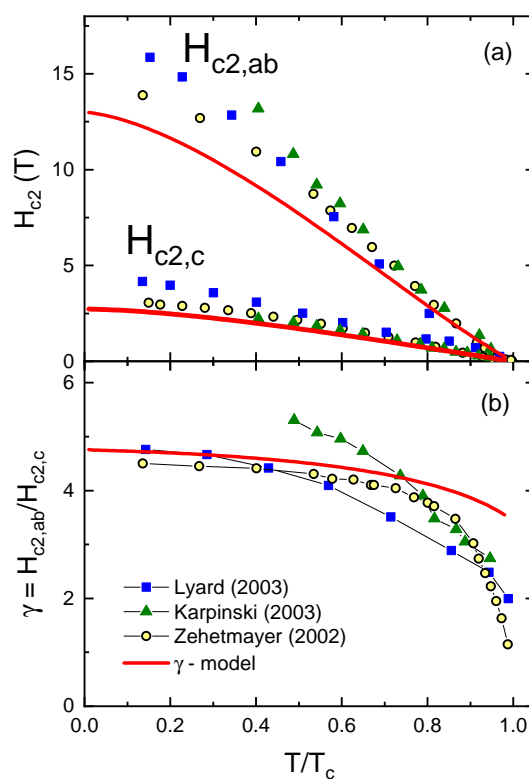


Figure 5. (a) Temperature dependent upper critical field $H_{c2}(T)$ in MgB_2 with the applied magnetic fields H_{dc} along ab -axis and c -axis. (b) Temperature dependent H_{c2} anisotropy $\gamma(T) = H_{c2,ab}(T)/H_{c2,c}(T)$. Solid line represent a calculated result by using γ model [32] and symbols are experimental results by Lyard et al. (squares) [41], Karpinski et al. (triangles) [42], and Zehetmayer et al. (circles) [43], respectively.

3. Materials and Methods

High quality single crystals of MgB_2 have been grown using a cubic, multianvil press, with an edge length of 19 mm from the Rockland Research Corporation (West Nyack, NY, USA). Pure distilled Mg (4 N) was squeezed so as to obtain a cylinder shaped ingot and placed into a boron nitride (BN) crucible. Enriched ^{11}B powder (4 N) was added into the crucible in 0.5 to 1 ratio with Mg. The crucible was then filled with BN powder. The synthesis was carried out in a high pressure furnace at a pressure of 3.3 GPa to grow high quality of MgB_2 single crystals out of the Mg solvent. The materials were heated up to 1500 °C over 1 h and held there for 4 h. The temperature was then slowly reduced to 700 °C at 2.7 °C/min. The furnace was stopped resulting in a fast cooling to room temperature. After releasing the pressure, the remaining Mg was distilled and single crystals of MgB_2 were obtained and manually separated from BN crystals. Typical samples are shiny platelets with dimensions of about $1 \times 0.5 \times 0.1 \text{ mm}^3$. In this paper, a sample with dimensions of $1.1 \times 0.4 \times 0.1 \text{ mm}^3$ was extracted and used for dc magnetization and the London penetration depth λ . The dc magnetization was measured in a quantum design magnetic property measurement system (MPMS) with an applied dc magnetic field of $H = 10 \text{ Oe}$. Temperature variation of London penetration depth $\Delta\lambda(T)$ was measured by using a tunnel-diode resonator (TDR) technique [24,44–46] which is mounted on a conventional ^3He cryostat with a base temperature as low as $T_{\text{min}} = 0.4 \text{ K}$. A LC tank circuit of TDR self-resonates at a frequency about $f_0 = 14 \text{ MHz}$ with an excitation ac magnetic field of $H_{ac} = 20 \text{ mOe}$ in the inductor coil. Placing a sample into the inductor causes the shift of the resonant frequency, $\Delta f(T) = -G4\pi\chi_{ac}(T)$ where G is a calibration constant determined by physically pulling the sample out of the inductor coil. With the characteristic sample size, R , $4\pi\chi_{ac} = (\lambda/R) \tanh(R/\lambda) - 1$, from which $\Delta\lambda(T)$ can be obtained [24,45,46].

4. Summary

A self-consistent γ -model with two isotropic s-wave gaps was used to describe several superconducting properties of MgB_2 based on the known electronic structure and pairing matrix obtained from the least squares fit to the experimental superfluid density $\rho_s(T) = \lambda^2(0)/\lambda^2(T)$. The temperature variation of the London penetration depth $\lambda(T)$ was measured using the tunnel diode resonator technique down to $0.01T_c$. Using the obtained single set of fitting parameters, the thermodynamic quantities including specific heat and upper critical field were calculated, and the temperature dependence of order parameters is in good agreement with the spectroscopic tunneling experiments. Our results provide solid experimental ground to using a sufficiently simple, yet self-consistent γ -model for the description of multigap superconductivity.

Author Contributions: Data curation, H.K., V.T., S.K.K., V.G.K. and R.P.; formal analysis, H.K., K.C., V.T. and S.K.K.; funding acquisition, P.C.C. and R.P.; supervision, P.C.C. and R.P.; validation, M.A.T., S.L.B., P.C.C., V.G.K. and R.P.; writing—original draft, H.K., K.C., V.T. and R.P.; writing—review and editing, H.K., K.C., M.A.T., S.L.B., P.C.C., V.G.K. and R.P.

Funding: This work was supported by the U.S. Department of Energy, Office of Basic Energy Science, Division of Materials Sciences and Engineering. The research was performed at the Ames Laboratory. Ames Laboratory is operated for the U.S. Department of Energy by Iowa State University under Contract No. DE-AC02-07CH11358.

Conflicts of Interest: The authors declare no conflict of interest. The funders had no role in the design of the study; in the collection, analyses, or interpretation of data; in the writing of the manuscript, or in the decision to publish the results.

Abbreviations

The following abbreviations are used in this manuscript:

TDR	Tunnel diode resonator
ARPES	Angle-resolved photoemission spectroscopy
FC	Field-cooled
ZFC	Zero-field-cooled
MPMS	Magnetic property measurement system

References

1. Nagamatsu, J.; Nakagawa, N.; Muranaka, T.; Zenitani, Y.; Akimitsu, J. Superconductivity at 39 K in magnesium diboride. *Nature* **2001**, *410*, 63. [[CrossRef](#)] [[PubMed](#)]
2. Bardeen, J.; Cooper, L.N.; Schrieffer, J.R. Theory of Superconductivity. *Phys. Rev.* **1957**, *108*, 1175–1204. [[CrossRef](#)]
3. Xi, X.X. Two-band superconductor magnesium diboride. *Rep. Prog. Phys.* **2008**, *71*, 116501. [[CrossRef](#)]
4. Bud'ko, S.L.; Canfield, P.C. Superconductivity of magnesium diboride. *Phys. C Supercond. Appl.* **2015**, *514*, 142–151. [[CrossRef](#)]
5. Bud'ko, S.L.; Lapertot, G.; Petrovic, C.; Cunningham, C.E.; Anderson, N.; Canfield, P.C. Boron Isotope Effect in Superconducting MgB₂. *Phys. Rev. Lett.* **2001**, *86*, 1877–1880. [[CrossRef](#)] [[PubMed](#)]
6. Hinks, D.G.; Claus, H.; Jorgensen, J.D. The complex nature of superconductivity in MgB₂ as revealed by the reduced total isotope effect. *Nature* **2001**, *411*, 457. [[CrossRef](#)] [[PubMed](#)]
7. Hinks, D.; Jorgensen, J. The isotope effect and phonons in MgB₂. *Phys. C Supercond.* **2003**, *385*, 98–104. [[CrossRef](#)]
8. Tajima, T. Possibility of MgB₂ application to superconducting cavities. In Proceedings of the Eighth European Particle Accelerator Conference, Paris, France, 3–7 June 2002; Los Alamos National Lab: Santa Fe, NM, USA, 2002.
9. Kalhor, S.; Ghanaatshoar, M.; Kashiwagi, T.; Kadowaki, K.; Kelly, M.J.; Delfanazari, K. Thermal Tuning of High-*T_c* Superconducting Bi₂Sr₂CaCu₂O_{8+δ} Terahertz Metamaterial. *IEEE Photonics J.* **2017**, *9*, 1–8. [[CrossRef](#)]
10. Delfanazari, K.; Puddy, R.K.; Ma, P.; Yi, T.; Cao, M.; Gul, Y.; Farrer, I.; Ritchie, D.A.; Joyce, H.J.; Kelly, M.J.; et al. On-Chip Andreev Devices: Hard Superconducting Gap and Quantum Transport in Ballistic Nb–In_{0.75}Ga_{0.25}As–Quantum-Well–Nb Josephson Junctions. *Adv. Mater.* **2017**, *29*, 1701836. [[CrossRef](#)]
11. Padamsee, H.; Neighbor, J.E.; Shiffman, C.A. Quasiparticle phenomenology for thermodynamics of strong-coupling superconductors. *J. Low Temp. Phys.* **1973**, *12*, 387–411. [[CrossRef](#)]
12. Bouquet, F.; Fisher, R.A.; Phillips, N.E.; Hinks, D.G.; Jorgensen, J.D. Specific Heat of Mg¹¹B₂: Evidence for a Second Energy Gap. *Phys. Rev. Lett.* **2001**, *87*, 047001. [[CrossRef](#)] [[PubMed](#)]
13. Bouquet, F.; Wang, Y.; Fisher, R.A.; Hinks, D.G.; Jorgensen, J.D.; Junod, A.; Phillips, N.E. Phenomenological two-gap model for the specific heat of MgB₂. *EPL Europhys. Lett.* **2001**, *56*, 856. [[CrossRef](#)]
14. Choi, H.J.; Roundy, D.; Sun, H.; Cohen, M.L.; Louie, S.G. The origin of the anomalous superconducting properties of MgB₂. *Nature* **2002**, *418*, 758. [[CrossRef](#)] [[PubMed](#)]
15. Fisher, R.; Li, G.; Lashley, J.; Bouquet, F.; Phillips, N.; Hinks, D.; Jorgensen, J.; Crabtree, G. Specific heat of Mg¹¹B₂. *Phys. C Supercond.* **2003**, *385*, 180–191. [[CrossRef](#)]
16. Panagopoulos, C.; Rainford, B.D.; Xiang, T.; Scott, C.A.; Kambara, M.; Inoue, I.H. Penetration depth measurements in MgB₂: Evidence for unconventional superconductivity. *Phys. Rev. B* **2001**, *64*, 094514. [[CrossRef](#)]
17. Niedermayer, C.; Bernhard, C.; Holden, T.; Kremer, R.K.; Ahn, K. Muon spin relaxation study of the magnetic penetration depth in MgB₂. *Phys. Rev. B* **2002**, *65*, 094512. [[CrossRef](#)]
18. Carrington, A.; Manzano, F. Magnetic penetration depth of MgB₂. *Phys. C Supercond.* **2003**, *385*, 205–214. [[CrossRef](#)]
19. Mou, D.; Jiang, R.; Taufour, V.; Bud'ko, S.L.; Canfield, P.C.; Kaminski, A. Momentum dependence of the superconducting gap and in-gap states in MgB₂ multiband superconductor. *Phys. Rev. B* **2015**, *91*, 214519. [[CrossRef](#)]
20. Mou, D.; Jiang, R.; Taufour, V.; Flint, R.; Bud'ko, S.L.; Canfield, P.C.; Wen, J.S.; Xu, Z.J.; Gu, G.; Kaminski, A. Strong interaction between electrons and collective excitations in the multiband superconductor MgB₂. *Phys. Rev. B* **2015**, *91*, 140502. [[CrossRef](#)]
21. Mou, D.; Manni, S.; Taufour, V.; Wu, Y.; Huang, L.; Bud'ko, S.L.; Canfield, P.C.; Kaminski, A. Isotope effect on electron-phonon interaction in the multiband superconductor MgB₂. *Phys. Rev. B* **2016**, *93*, 144504. [[CrossRef](#)]
22. Manzano, F.; Carrington, A.; Hussey, N.E.; Lee, S.; Yamamoto, A.; Tajima, S. Exponential Temperature Dependence of the Penetration Depth in Single Crystal MgB₂. *Phys. Rev. Lett.* **2002**, *88*, 047002. [[CrossRef](#)] [[PubMed](#)]

23. Ding, H.; Richard, P.; Nakayama, K.; Sugawara, K.; Arakane, T.; Sekiba, Y.; Takayama, A.; Souma, S.; Sato, T.; Takahashi, T.; et al. Observation of Fermi-surface dependent nodeless superconducting gaps in $\text{Ba}_{0.6}\text{K}_{0.4}\text{Fe}_2\text{As}_2$. *EPL Europhys. Lett.* **2008**, *83*, 47001. [[CrossRef](#)]
24. Prozorov, R.; Kogan, V.G. London penetration depth in iron-based superconductors. *Rep. Prog. Phys.* **2011**, *74*, 124505. [[CrossRef](#)]
25. Hirschfeld, P.J.; Korshunov, M.M.; Mazin, I.I. Gap symmetry and structure of Fe-based superconductors. *Rep. Prog. Phys.* **2011**, *74*, 124508. [[CrossRef](#)]
26. Chubukov, A. Pairing Mechanism in Fe-Based Superconductors. *Annu. Rev. Condens. Matter Phys.* **2012**, *3*, 57–92. [[CrossRef](#)]
27. Seyfarth, G.; Brison, J.P.; Knebel, G.; Aoki, D.; Lapertot, G.; Flouquet, J. Multigap Superconductivity in the Heavy-Fermion System CeCoIn_5 . *Phys. Rev. Lett.* **2008**, *101*, 046401. [[CrossRef](#)] [[PubMed](#)]
28. Ruby, M.; Heinrich, B.W.; Pascual, J.I.; Franke, K.J. Experimental Demonstration of a Two-Band Superconducting State for Lead Using Scanning Tunneling Spectroscopy. *Phys. Rev. Lett.* **2015**, *114*, 157001. [[CrossRef](#)] [[PubMed](#)]
29. Golubov, A.A.; Kortus, J.; Dolgov, O.V.; Jepsen, O.; Kong, Y.; Andersen, O.K.; Gibson, B.J.; Ahn, K.; Kremer, R.K. Specific heat of MgB_2 in a one- and a two-band model from first-principles calculations. *J. Phys. Condens. Matter* **2002**, *14*, 1353. [[CrossRef](#)]
30. Floris, A.; Profeta, G.; Lathiotakis, N.N.; Lüders, M.; Marques, M.A.L.; Franchini, C.; Gross, E.K.U.; Continenza, A.; Massidda, S. Superconducting Properties of MgB_2 from First Principles. *Phys. Rev. Lett.* **2005**, *94*, 037004. [[CrossRef](#)]
31. Eilenberger, G. Transformation of Gorkov's equation for type II superconductors into transport-like equations. *Zeitschrift für Physik A Hadrons and Nuclei* **1968**, *214*, 195–213. [[CrossRef](#)]
32. Kogan, V.G.; Martin, C.; Prozorov, R. Superfluid density and specific heat within a self-consistent scheme for a two-band superconductor. *Phys. Rev. B* **2009**, *80*, 014507. [[CrossRef](#)]
33. Li, M.; Lee-Hone, N.R.; Chi, S.; Liang, R.; Hardy, W.N.; Bonn, D.A.; Girt, E.; Broun, D.M. Superfluid density and microwave conductivity of FeSe superconductor: Ultra-long-lived quasiparticles and extended s-wave energy gap. *New J. Phys.* **2016**, *18*, 082001. [[CrossRef](#)]
34. Kim, H.; Kogan, V.G.; Cho, K.; Tanatar, M.A.; Prozorov, R. Rutgers relation for the analysis of superfluid density in superconductors. *Phys. Rev. B* **2013**, *87*, 214518. [[CrossRef](#)]
35. Ohishi, K.; Muranaka, T.; Akimitsu, J.; Koda, A.; Higemoto, W.; Kadono, R. Quasiparticle Excitations outside the Vortex Cores in MgB_2 Probed by Muon Spin Rotation. *J. Phys. Soc. Jpn.* **2003**, *72*, 29–32. [[CrossRef](#)]
36. Kim, H.; Tanatar, M.A.; Song, Y.J.; Kwon, Y.S.; Prozorov, R. Nodeless two-gap superconducting state in single crystals of the stoichiometric iron pnictide LiFeAs . *Phys. Rev. B* **2011**, *83*, 100502. [[CrossRef](#)]
37. Belashchenko, K.D.; Schilfgaarde, M.V.; Antropov, V.P. Coexistence of covalent and metallic bonding in the boron intercalation superconductor MgB_2 . *Phys. Rev. B* **2001**, *64*, 092503. [[CrossRef](#)]
38. Chen, K.; Cui, Y.; Li, Q.; Zhuang, C.G.; Liu, Z.K.; Xi, X.X. Study of MgB_2 I Pb tunnel junctions on MgO (211) substrates. *Appl. Phys. Lett.* **2008**, *93*, 012502. [[CrossRef](#)]
39. Putti, M.; Affronte, M.; Ferdeghini, C.; Manfrinetti, P.; Tarantini, C.; Lehmann, E. Observation of the Crossover from Two-Gap to Single-Gap Superconductivity through Specific Heat Measurements in Neutron-Irradiated MgB_2 . *Phys. Rev. Lett.* **2006**, *96*, 077003. [[CrossRef](#)]
40. Kogan, V.G.; Prozorov, R. Orbital upper critical field and its anisotropy of clean one- and two-band superconductors. *Rep. Prog. Phys.* **2012**, *75*, 114502. [[CrossRef](#)]
41. Lyard, L.; Samuely, P.; Szabó, P.; Marcenat, C.; Klein, T.; Kim, K.H.P.; Jung, C.U.; Lee, H.S.; Kang, B.; Choi, S.; et al. Upper critical magnetic fields in single crystal MgB_2 . *Supercond. Sci. Technol.* **2003**, *16*, 193. [[CrossRef](#)]
42. Karpinski, J.; Angst, M.; Jun, J.; Kazakov, S.M.; Puzniak, R.; Wisniewski, A.; Roos, J.; Keller, H.; Perucchi, A.; Degiorgi, L.; et al. MgB_2 single crystals: High pressure growth and physical properties. *Supercond. Sci. Technol.* **2003**, *16*, 221. [[CrossRef](#)]
43. Zehetmayer, M.; Eisterer, M.; Jun, J.; Kazakov, S.M.; Karpinski, J.; Wisniewski, A.; Weber, H.W. Mixed-state properties of superconducting MgB_2 single crystals. *Phys. Rev. B* **2002**, *66*, 052505. [[CrossRef](#)]
44. Van Degrift, C.T. Tunnel diode oscillator for 0.001 ppm measurements at low temperatures. *Rev. Sci. Instrum.* **1975**, *46*, 599–607. [[CrossRef](#)]

45. Prozorov, R.; Giannetta, R.W.; Carrington, A.; Araujo-Moreira, F.M. Meissner-London state in superconductors of rectangular cross section in a perpendicular magnetic field. *Phys. Rev. B* **2000**, *62*, 115–118. [[CrossRef](#)]
46. Cho, K.; Kończykowski, M.; Teknowijoyo, S.; Tanatar, M.A.; Prozorov, R. Using electron irradiation to probe iron-based superconductors. *Supercond. Sci. Technol.* **2018**, *31*, 064002. [[CrossRef](#)]



© 2019 by the authors. Licensee MDPI, Basel, Switzerland. This article is an open access article distributed under the terms and conditions of the Creative Commons Attribution (CC BY) license (<http://creativecommons.org/licenses/by/4.0/>).